ORIGINAL ARTICLE

Preoperative F-18 fluorocholine PET/CT for the detection of hyperfunctioning parathyroid glands in patients with secondary or tertiary hyperparathyroidism: comparison with Tc-99m sestamibi scan and neck ultrasound

Yu-Hung Chen[1] · Hwa-Tsung Chen[2] · Ming-Che Lee[2] · Shu-Hsin Liu[1,3] · Ling-Yi Wang[4,5] · Kun-Han Lue[3] · Sheng-Chieh Chan[1]

Abstract

Objectives Currently, neck ultrasound is the preferred preoperative imaging in patients with secondary/tertiary hyperparathyroidism, and the use of Tc-99m sestamibi scan is limited in these patients. We conducted this study to compare the diagnostic utilities of F-18 fluorocholine PET/CT, Tc-99m sestamibi scintigraphy, and neck ultrasound for localizing hyperfunctioning parathyroid glands in secondary/tertiary hyperparathyroidism.

Methods We prospectively enrolled 30 dialysis patients with a diagnosis of secondary/tertiary hyperparathyroidism; of these, 27 participants underwent all three imaging modalities, including dual-phase F-18 fluorocholine PET/CT (PET acquired 5 and 60 min after tracer injection), dual-phase Tc-99 m sestamibi SPECT/CT, and neck ultrasound. All patients underwent parathyroidectomy after imaging. We compared the lesion-based sensitivity, specificity, and accuracy of the three image tools using histopathology as the reference.

Results A total of 27 patients (107 lesions) underwent all three imaging modalities and entered the final analysis. The lesion-based sensitivities of F-18 fluorocholine PET/CT, Tc-99m sestamibi, and ultrasound were 86%, 55%, and 62%, respectively (both $p < 0.001$, when comparing F-18 fluorocholine PET/CT to Tc-99 m sestamibi scan and to ultrasound). F-18 fluorocholine PET/CT, Tc-99m sestamibi, and ultrasound had similar specificities of 93%, 80%, and 87%, respectively. The accuracy of F-18 fluorocholine PET/CT (87%) was significantly higher than that of Tc-99m sestamibi (59%) and ultrasound (65%) (both $p < 0.001$). F-18 fluorocholine PET/CT identified more hyperplastic glands than ultrasound in 52% (14/27) patients. The sensitivity of F-18 fluorocholine PET/CT reached 95% for hyperplastic parathyroid masses as low as 200 mg.

Conclusions F-18 fluorocholine PET/CT shows superior accuracy over the conventional imaging modalities in patients with secondary or tertiary hyperparathyroidism. The combination of F-18 fluorocholine PET/CT and neck ultrasound may enable better surgical planning in these patients.

Registration identification number NCT04316845.

Keywords F-18 fluorocholine · Positron emission tomography · Tc-99m sestamibi · Ultrasound · Secondary hyperparathyroidism

Introduction

Hyperparathyroidism is the third most common endocrine disorder in which an elevated serum intact parathyroid hormone (iPTH) is detected [1]. It can result from an autonomous hyperfunctioning parathyroid adenoma or secondary due to chronic kidney dysfunction. End-stage renal disease is a major cause of secondary or tertiary hyperparathyroidism. Among patients with end-stage renal disease, 12–54% have

✉ Sheng-Chieh Chan
williamsm.tw@gmail.com

Extended author information available on the last page of the article

hyperparathyroidism [2]. Secondary/tertiary hyperparathyroidism is especially prevalent in regions with a high dialysis prevalence, for example, in Asian countries such as Taiwan [3, 4]. Uncontrolled hyperparathyroidism can lead to lethal cardiovascular and neuropsychiatric complications [5, 6]. The initial management of secondary or tertiary hyperparathyroidism is medical [7]. However, parathyroidectomies are needed for patients with iPTH values over 1000 pg/mL or symptoms such as pruritus [8, 9]. Because parathyroid glands are relatively small and located near-critical neurovascular structures, accurate preoperative localization is important.

Although Tc-99m sestamibi scintigraphy or neck ultrasound is often used for detecting hyperfunctioning glands in primary hyperparathyroidism, their accuracies were suboptimal in secondary or tertiary hyperparathyroidism. Tc-99m sestamibi images have low sensitivity in patients with multiglandular disease or hyperplasia, which are common in secondary or tertiary hyperparathyroidism [10–17]. Ultrasonography of the neck depends heavily on operator skills and demonstrates widely variable sensitivity (ranging from 30 to 80%) in individuals with secondary or tertiary hyperparathyroidism [18]. Therefore, a more reliable imaging tool for preoperative localization of hyperfunctioning glands in patients with secondary or tertiary hyperparathyroidism is needed.

Recently, studies using positron emission tomography (PET) with radioactive choline such as C-11 choline or F-18 fluorocholine have shown promising results for detecting parathyroid adenomas in patients with primary hyperparathyroidism [19–24]. However, those studies were done in patients with primary hyperparathyroidism or mixed cohorts. Unlike patients with primary hyperparathyroidism, those with secondary hyperparathyroidism exhibit more multiglandular diseases and supernumerary or ectopic glands [25], which have been associated with deteriorated diagnostic performance of the nuclear medicine test. For example, the sensitivities of Tc-99m sestamibi scintigraphy for primary and secondary hyperparathyroidism have been reported to be 88% and 44%, respectively [16, 17, 26, 27]. Thus, further investigation of the diagnostic performance of choline PET in patients with secondary hyperparathyroidism is necessary.

This prospective study aims to investigate the performance of F-18 fluorocholine PET for the preoperative localization of hyperplastic parathyroid glands in secondary/tertiary hyperparathyroidism due to chronic renal dysfunction. We also compared the performance with those of Tc-99m sestamibi scintigraphy and neck ultrasound.

Materials and methods

Study population

The local institutional review board and ethics committee approved the protocol used in our prospective study. We obtained written informed consents from all study participants. We performed the study between January 2018 and December 2019. The inclusion criteria were as follows: (a) patients receiving dialysis for chronic renal dysfunction and diagnosed as having hyperparathyroidism (serum iPTH exceeded 80 pg/mL) and (b) patients scheduled to receive parathyroidectomy due to iPTH values over 1000 pg/mL or presence of symptoms such as pruritus despite medical treatment. We established a diagnosis of tertiary hyperparathyroidism in patients with serum calcium concentration exceeding 2.65 mmol/L [7]. We excluded patients with primary hyperparathyroidism and those who were not able to tolerate the F-18 fluorocholine PET/CT procedures. A total of 30 patients with secondary or tertiary hyperparathyroidism were included in this study. Table 1 summarizes the general characteristics of these patients. The enrolled patients were scheduled to receive F-18 fluorocholine PET/CT, Tc-99m sestamibi scan, and neck ultrasound before parathyroidectomy.

F-18 fluorocholine PET/CT imaging protocol

No fasting was required before F-18 fluorocholine PET imaging. We administered $185 \pm 10\%$ MBq of intravenous F-18 fluorocholine. Patients were positioned supine with their arms placed on their sides. Images were acquired 5 (early image) and 60 min (delayed image) after the radiotracer injection [28–31]. The field of view covered at least from the skull base to the liver. The scans were performed using a GE Discovery ST PET/CT unit (Discovery ST16; GE Healthcare, Milwaukee, WI, USA). The PET/CT system was equipped with a 16-detector row (912 detectors/row) transmission CT unit and a PET component with 10,080 bismuth germanate crystals in 24 rings. A transmission CT scan was obtained first using a tube voltage and tube current of 120 kV and 120 mA, respectively. The pitch was 1.75. Image sampling was conducted using the helical mode with a 3.75-mm helical thickness. The image reconstruction matrices were 512×512. We acquired all transmission CT images without the administration of any iodinated contrast material. We obtained PET emission images with 3.0 min of scanning time per table position (15 cm per table position with a 3-cm overlap for every contiguous frame). The PET images were reconstructed with CT for attenuation correction, and we

Table 1 Distribution of baseline patient characteristics ($n = 30$)

Variable	Value
Age (years), mean ± SD	49.5 ± 14.11
Gender, *n* (%)	
Male	19 (63.3)
Female	11 (36.7)
Diagnosis, *n* (%)	
Secondary hyperparathyroidism	23 (76.7)
Tertiary hyperparathyroidism	7 (23.3)
Preoperative serum phosphate (mg/dL), mean ± SD	5.6 ± 1.62
Preoperative serum calcium (mmol/L), mean ± SD	
Secondary hyperparathyroidism	2.4 ± 0.22
Tertiary hyperparathyroidism	2.8 ± 0.13
Method of renal replacement therapy, *n* (%)	
Hemodialysis	25 (83.3)
Peritoneal dialysis	5 (16.7)
Previous parathyroidectomy, *n* (%)	
Presence	4 (13.3)
Absence	26 (86.7)
Time from imaging to surgery (day), median (IQR)	6.5 (18)
Surgical procedure, *n* (%)	
Total parathyroidectomy	19 (63.4)
Subtotal parathyroidectomy	9 (30.0)
Resection of mediastinal ectopic gland	1 (3.3)
Resection of graft gland[a]	1 (3.3)
iPTH level (pg/mL), mean ± SD	
Preoperative value	1655.2 ± 742.23
Postoperative value	249.4 ± 188.82
Reduction ratio of iPTH at 15 min, median (IQR)	0.88 (0.09)
Number of patients with multiglandular disease	27 (90%)
Weight of parathyroid gland (mg), median (IQR)[b]	577 (836.75)

SD standard deviation, *iPTH* intact parathyroid hormone, *IQR* interquartile range

[a] Graft gland in the left brachialis muscle pouch

[b] Data were not available in two glands because of ruptures during parathyroidectomy

used an ordered subset expectation maximization iterative reconstruction algorithm (two iterations and 21 subsets; matrix size, 128×128).

PET image interpretation and analysis

The F-18 fluorocholine PET image data were visually evaluated in consensus by two nuclear medicine physicians. The readers were aware of the study protocol, but were blinded to the results of the other imaging modalities. Focal radiotracer uptakes in the anterior neck or mediastinum were determined to be positive for hyperfunctioning parathyroid tissue. The interpreters reported the number of abnormal glands and the location of each abnormal parathyroid gland (right upper thyroid bed, right lower thyroid bed, left upper thyroid bed, left lower thyroid bed, ectopic, or graft site). We also analyzed the F-18 fluorocholine PET semiquantitatively using the PMOD 4.0 software package (PMOD Technologies, Zurich, Switzerland). An experienced nuclear medicine physician drew the volumes-of-interest (VOI) to calculate the standardized uptake values (SUV). The SUV was calculated based on the following formula: SUV = (decay-corrected activity [kBq] per milliliter of tissue volume)/ (injected F-18 fluorocholine activity [kBq]/body weight in g). The VOIs were placed on the parathyroid lesions. We also drew VOI for the whole thyroid lobe on the PET image to obtain the mean SUV of the thyroid background. We first selected the transaxial slide that showed the largest thyroid section and then manually drew the VOI to include the entire thyroid section. We drew a total of three thyroid slides to create the thyroid VOI. We calculated the parathyroid-to-thyroid uptake ratio (*P/T*) according to the following formula: (SUVmax of the parathyroid lesion)/(mean SUV of the thyroid gland).

Single-isotope dual-phase Tc-99 m sestamibi scan and image interpretation

We administered $925 \pm 10\%$ MBq of intravenous Tc-99m sestamibi to all the patients. Early and delayed anterior planar images with 1 million counts were acquired 15 min and 2–4 h after the radiotracer injection. The image fields included the neck and mediastinum. We also obtained a focal magnified image of the neck with a zoom factor of 3. We acquired a SPECT/CT with the field of view that included the neck and the mediastinum after the delayed planar images were done. The Tc-99m sestamibi scans were done on a GE Infinia Hawkeye SPECT/CT system (Infinia Hawkeye 4; GE Healthcare, Milwaukee, WI, USA) equipped with a low-energy high-resolution parallel holed collimator. The SPECT/CT protocol was the following: we obtained a transmission CT scan first with the tube voltage and current set at 140 kV and 2.5 mA, respectively. The image sampling was conducted using the axial mode with a slice thickness of 5 mm. No iodinated contrast material was administered. The emission scan with 90 projections (4-degree interval) of 16 s each was obtained after the transmission scan. The SPECT images were reconstructed by an ordered subset expectation maximization algorithm with ten subsets and two iterations. The reconstruction matrices were 128×128. We used a Butterworth post-reconstruction filter with a critical frequency and a power of 0.5 and 10, respectively. We did not apply scatter correction for any SPECT images, nor did we attempt to correct the partial volume effect. The planar images and SPECT/CT scan were displayed using the manufacturer software on the Xeleris 2.1753 Workstation (GE Healthcare, Milwaukee, Wisconsin, USA). The interpretation of Tc-99m

sestamibi images was made in consensus by two nuclear medicine physicians. The readers were blinded to the results of the other imaging modalities. We considered focal radiotracer uptakes that became more discernible with a better contrast to thyroid bed background in delayed images as positive. Focal radiotracer uptakes in the delayed planar scan or in the SPECT were also determined to be positive. The interpreters recorded the number and location of abnormal parathyroid glands.

Ultrasound of the neck

An experienced surgeon performed the neck ultrasound in the outpatient clinic. The ultrasound was performed with a Flex Focus 400 ultrasound system (BK Medical, Herlev, Denmark) using a linear transducer (frequency of 5–12 MHz, Linear Array 8811, BK Medical, Herlev, Denmark). Each patient was placed in the supine position with neck hyperextension. The longitudinal and axial ultrasonographic images were obtained from bilateral mandibular angles to the sternal notch, and laterally to include the jugular veins. The surgeon searched for the parathyroid glands in relation to the upper and lower poles of the bilateral thyroid lobes, and recorded the number of parathyroid gland(s) and their location (right upper thyroid bed, right lower thyroid bed, left upper thyroid bed, and left lower thyroid bed).

Parathyroidectomy

Surgeons performed parathyroidectomies under general anesthesia. Both sides of the neck including the bilateral paratracheal, tracheoesophageal groove, and upper anterior mediastinal spaces were thoroughly explored. All the identified abnormal parathyroid glands were removed in either subtotal or total parathyroidectomies. In cases in which subtotal parathyroidectomy was selected, half of the smallest parathyroid gland was left in situ. The weight of all the resected parathyroid glands was recorded. Hyperplastic parathyroid tissues were removed under ultrasound guidance from the graft site in patients with suspected graft parathyroid tissue hyperplasia (in the subcutaneous pouch or muscle pouch of the forearm). In a patient with suspected ectopic parathyroid hyperplasia in the mediastinum, an experienced thoracic surgeon performed the surgery. The ectopic gland was explored and resected using a video-assisted thoracoscopic procedure through the third left intercostal space. Serum iPTH levels were checked 15 min after completion of the parathyroidectomies. We considered decrease ratios of 0.8 or more from the baseline serum iPTH levels at 15 min as indicating successful parathyroidectomies [32, 33]. Histopathological examination of the resected specimens was used to confirm the presence of parathyroid tissue.

Statistical analysis

We presented patients' demographic data as frequencies, proportions, medians, or means depending on each variable's characteristics. We performed lesion-based instead of patient-based analyses for each imaging tool, because most patients with secondary or tertiary hyperparathyroidism had more than one hyperfunctioning parathyroid glands. For each image modality, we reported sensitivity, specificity, positive predictive value (PPV), negative predictive value (NPV), and accuracy using the histopathological examination as the reference standard. We considered glands as positive in cases with parathyroid hyperplasia on definitive histopathological exam. We performed McNemar's test to examine whether the performance (sensitivity, specificity, and accuracy) of F-18 fluorocholine PET/CT was different from those of the other two modalities. We examined whether the PPV and NPV differed between these three image tools using the Chi-square test. Also, we used the Mann–Whitney U test to compare the hyperplastic parathyroid gland weights between different imaging modalities. We examined the correlation between the semiquantitative PET values and the weight of parathyroid lesions by Spearman's correlation analysis. We compared semiquantitative values derived from early and delayed F-18 fluorocholine PET scans by paired t tests. We performed all statistical analyses using the SPSS software (version 20.0; SPSS Inc., Chicago, IL, USA). All the tests were two-sided and a p value of < 0.05 was considered statistically significant.

Results

Patients

All participants underwent parathyroidectomies after imaging. The median interval from F-18 fluorocholine PET/CT to parathyroidectomy was 6.5 days with an interquartile range (IQR) of 18 days. One patient's surgery was delayed (71 days after imaging) because of peritonitis. The median iPTH reduction ratio at 15 min after parathyroidectomy was 0.88 with an IQR of 0.09. All study participants underwent both F-18 fluorocholine PET/CT and Tc-99m sestamibi imaging. However, three patients refused to undergo the neck ultrasound examination; therefore, 27 patients underwent all three imaging modalities and were included in the final analysis.

Comparison of the diagnostic performance of the three imaging modalities

F-18 fluorocholine PET/CT, Tc-99m sestamibi, and ultrasound images revealed 80, 54, and 59 lesions, respectively.

We obtained 107 surgical specimens during the operations for the 27 participants, and 92 lesions were confirmed to be parathyroid hyperplasia. Table 2 summarizes the lesion-based diagnostic performances of the three imaging modalities. The sensitivity, specificity, PPV, NPV, and accuracy of F-18 fluorocholine PET/CT were 86%, 93%, 99%, 52%, and 87%, respectively. F-18 fluorocholine PET/CT has significantly higher sensitivity, NPV, and accuracy than Tc-99m sestamibi scan and neck ultrasound (Table 2 and Fig. 1). The sensitivities, specificities, PPVs, NPVs, and accuracies between Tc-99m sestamibi scans and neck ultrasounds were similar.

F-18 fluorocholine PET/CT, Tc-99m sestamibi scans, and neck ultrasounds identified 79, 51, and 57 true-positive hyperplastic glands, respectively. When comparing Tc-99m sestamibi scan with neck ultrasound (Electronic supplementary material 1), of the 57 hyperplastic glands detected by the neck ultrasound, 19 were not detected by the Tc-99m sestamibi scan. Conversely, of the 51 hyperplastic glands detected by the Tc-99m sestamibi scan, 13 were not detected by the neck ultrasound. The combination of Tc-99m sestamibi scan and neck ultrasound detected 70 hyperplastic glands. All parathyroid hyperplastic lesions detected on Tc-99m sestamibi scans were also positive on the F-18 fluorocholine PET/CT. All but four parathyroid lesions identified on the neck ultrasound were also positive on the F-18 fluorocholine PET/CT. In all, 83 hyperplastic parathyroid glands were detected by the combination of F-18 fluorocholine PET/CT and neck ultrasound. An ectopic gland in the superior mediastinum was detected by both F-18 fluorocholine PET/CT and Tc-99m sestamibi scan.

On the individual level, the F-18 fluorocholine PET/CT revealed more hyperplastic parathyroid glands than the Tc-99m sestamibi scans or neck ultrasounds in 59% (16/27) and 52% (14/27) of patients, respectively. All 27 patients had a successful operation with the iPTH reduction ratio exceeding 0.8, except for one patient (patient No. 3, a reoperated case with tertiary hyperparathyroidism). Figure 2 demonstrates a case that benefited from the additional PET/CT findings.

Association between diagnostic capacities of the imaging modalities and the clinical variables

The median and IQR of the weight of hyperplastic parathyroid glands in all patients were 577 mg and 836.75 mg (range 46–6646 mg). The median values (IQR) of the hyperplastic parathyroid lesions undetected on F-18 fluorocholine PET/CT, Tc-99m sestamibi scan and neck ultrasound were 150 mg (214.5 mg), 279 mg (459.5 mg), and 423 mg (723 mg), respectively. The weight of these undetected lesions in F-18 fluorocholine PET/CT was significantly lower than those in the other two image modalities ($p = 0.027$, Fig. 3). The sensitivity of F-18 fluorocholine PET/CT reached 95% in hyperplastic parathyroid glands as low as 200 mg.

The sensitivities of early and delayed F-18 fluorocholine PET/CT images were 80% and 83%, respectively ($p = 0.248$). The specificities, PPVs, NPVs, and the diagnostic accuracies were similar between early and delayed images (Electronic supplementary material 2). The diagnostic performances were similar between patients with secondary and tertiary hyperparathyroidism (Electronic supplementary material 3).

Semiquantitative parameters of F-18 fluorocholine PET

In the early images, the mean ± standard deviation (SD) of SUVmax and P/T in all parathyroid lesions was 3.4 ± 1.50 and 2.5 ± 0.91, respectively. The mean ± SD of lesion SUVmax and P/T in the delayed scans was 3.3 ± 1.70 and 2.7 ± 1.11, respectively. We found that the early and delayed SUVmax of the parathyroid lesions were similar. Nevertheless, the *P/T* increased significantly in the delayed images ($p < 0.001$). The correlation with diseased glandular weight was better using the *P/T* than the SUVmax of lesions (Electronic supplementary material 4).

Table 2 Lesion-based analysis of three imaging modalities (107 lesions in 27 patients)

Imaging tool	TP	FP	TN	FN	Sensitivity (%)	p^a	Specificity (%)	p^a	PPV (%)	p^a	NPV (%)	p^a	Accuracy (%)	p^a
F-18 fluorocholine PET/CT	79	1	14	13	86	NA	93	NA	99	NA	52	NA	87	NA
Tc-99m sestamibi SPECT/CT	51	3	12	41	55	< 0.001	80	NS	94	NS	23	0.008	59	< 0.001
Neck ultrasound	57	2	13	35	62	< 0.001	87	NS	97	NS	27	0.032	65	< 0.001

Excluding three patients who did not have available neck ultrasound data for analysis

PET positron emission tomography, *SPECT* single-photon emission tomography, *TP* true-positive, *FP* false positive, *TN* true negative, *FN* false negative, *PPV* positive predictive value, *NPV* negative predictive value, *NA* not applicable, *NS* not statistically significant
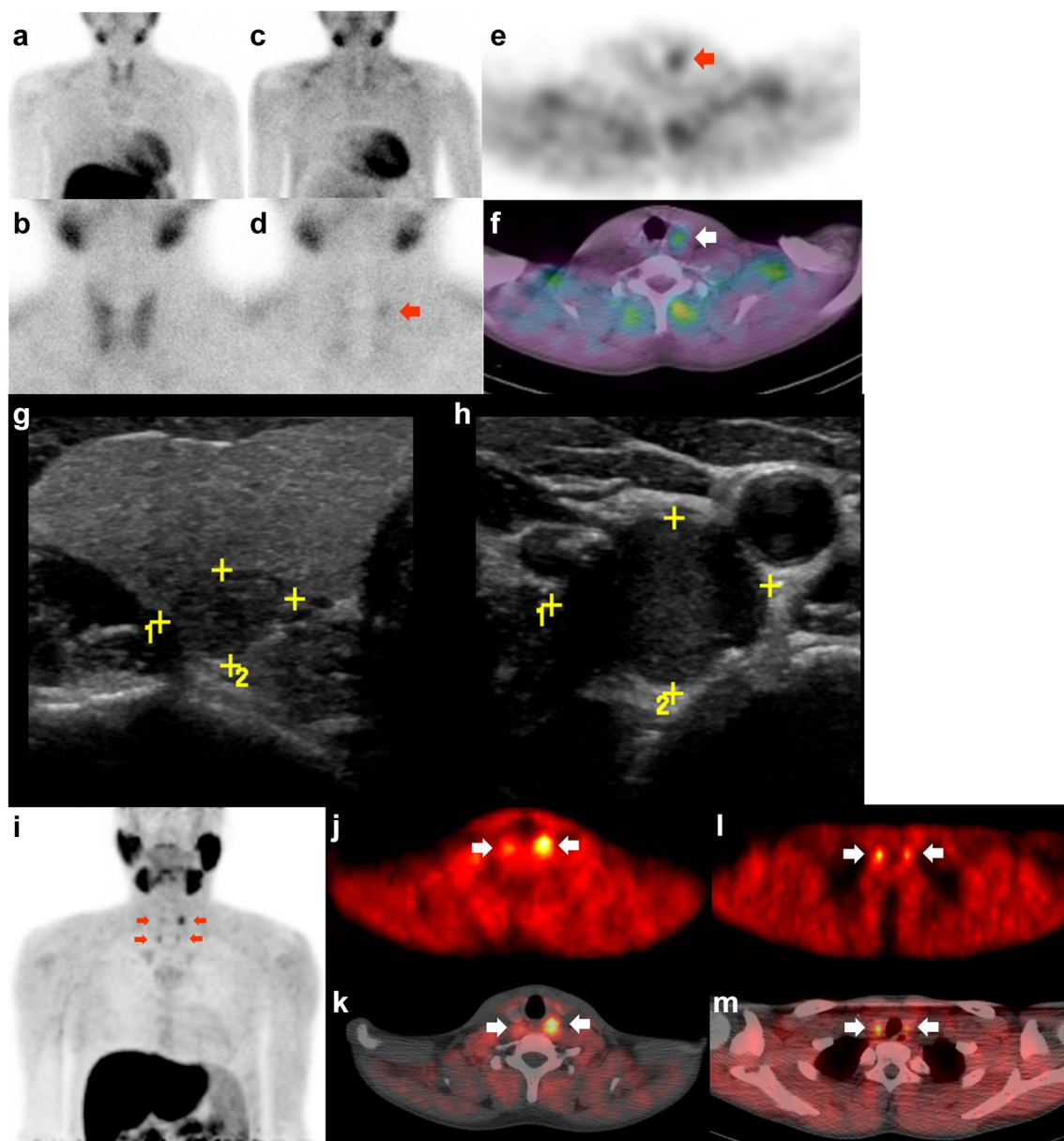
[a]Compared to F-18 fluorocholine PET/CT

Fig. 1 A 20-year-old man on peritoneal dialysis for 4 years was referred to us due to a serum iPTH level of 2281 pg/mL. The early (15 min after radiotracer injection, **a**, **b**) and delayed (2 h 10 min after the radiotracer injection, **c**, **d**) Tc-99 m sestamibi scans revealed focal tracer retention in the upper pole of the left thyroid lobe in the planar (**d**, red arrow) and SPECT/CT images (**e**, **f**), suggesting parathyroid hyperplasia. Neck ultrasound revealed the presence of enlarged lesions in the lower pole of the right thyroid lobe (**g**, 1.3 cm) and in the upper pole of the left thyroid lobe (**h**, 2 cm). The maximum inten- sity projection of F-18 fluorocholine PET revealed four well-discernible choline avid foci in the neck (**i**, red arrows). The transaxial images of PET/CT revealed that these lesions were located in the upper (**j**, **k**, white arrows) and lower (**l**, **m**, white arrows) poles of the bilateral thyroid lobes. The patient received subtotal parathyroidectomy and the postoperative iPTH level was 377 pg/mL (reduction ratio 83%). All four lesions showed parathyroid hyperplasia on pathological examination. *iPTH* intact parathyroid hormone

Discussion

Management of secondary or tertiary hyperparathyroidism is becoming a challenge along with the increasing prevalence of the chronic renal disease [2–4]. Because Tc-99m sestamibi scan has low sensitivity and adds limited information to neck ultrasound in this disease entity, it is not considered a clinical routine before parathyroidectomy [18, 26]. Our results showed that the F-18 fluorocholine PET/CT had a significantly higher sensitivity than that of Tc-99m sestamibi scan or neck ultrasound ($p < 0.001$) for detecting hyperplastic glands in patients with secondary or tertiary
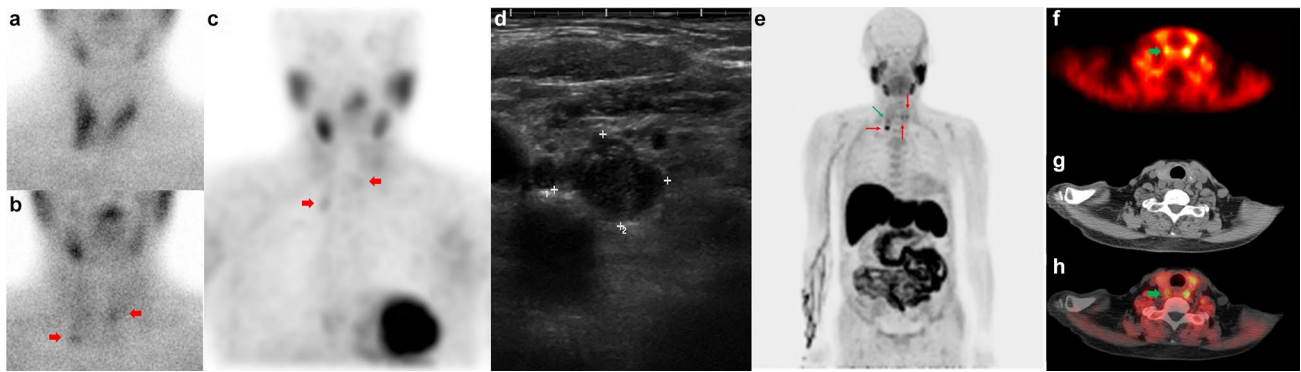
Fig. 2 F-18 fluorocholine PET/CT helps the surgeon to localize a small parathyroid lesion during parathyroidectomy. Representative imaging of a 74-year-old man on hemodialysis for 6 years and with a serum iPTH level of 1137 pg/mL. The early (15 min after radiotracer injection, **a**) and delayed (2 h after radiotracer injection, **b**) Tc-99 m sestamibi scan, and the MIP image of SPECT/CT (**c**) identified two suspected lesions in the lower pole of the right thyroid lobe and the upper pole of the left thyroid lobe (red arrows), suggesting parathyroid hyperplasia. Neck ultrasound only found a hypoechoic nodular lesion situated in the lower pole of right thyroid lobe (**d**), suggesting hyperplastic parathyroid gland. During the parathyroidectomy, the surgeon identified and removed a right lower parathyroid gland (630 mg), and two left parathyroid glands (335 mg and 105 mg) first. However, the right upper parathyroid gland (RUG) could not be identified during the surgical exploration of the right thyroid bed. The surgeon then reviewed the preoperative F-18 fluorocholine PET/CT, which revealed four suspected hyperplastic parathyroid glands on the MIP image (**e**, green and red arrows) and suggested that the RUG was located in the right trachea-esophageal groove (**f–h**, green arrows). The RUG was then identified and removed (122 mg). After the removal of the four parathyroid lesions, the iPTH level decreased to 87 pg/mL. *iPTH* intact parathyroid hormone, *MIP* maximum intensity projection

Fig. 3 Boxplot showing the weight of hyperplastic glands in false-negative lesions. The weight of false-negative glands on F-18 fluorocholine PET/CT was significantly lower than that on the Tc-99 m sestamibi scan and neck ultrasound ($p = 0.027$)
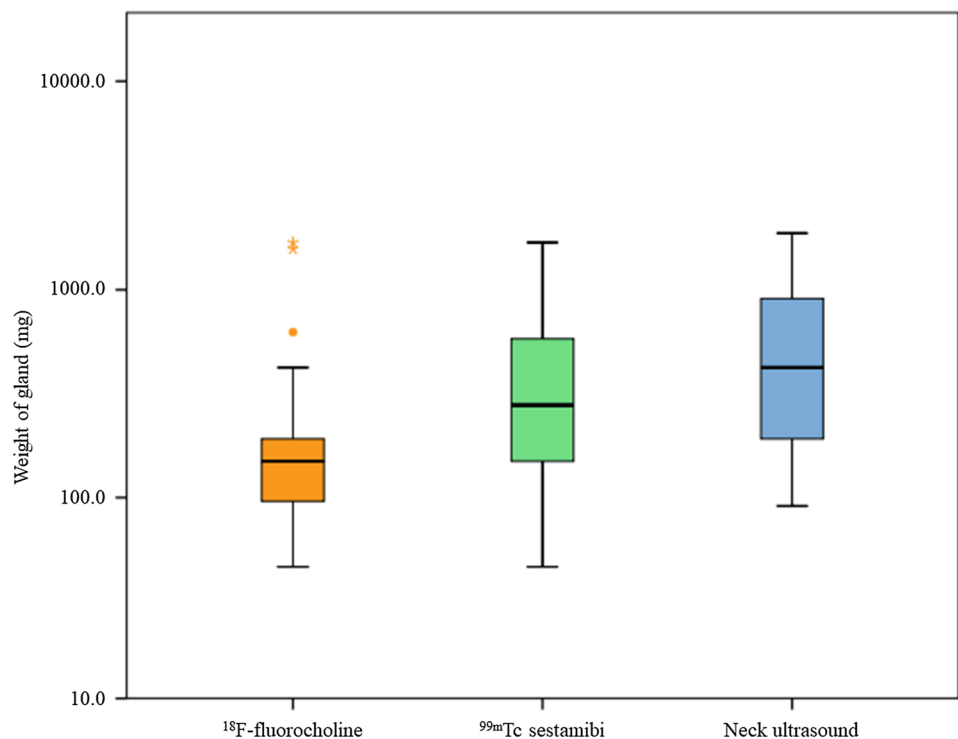
hyperparathyroidism. In addition, F-18 fluorocholine PET/CT revealed more hyperplastic parathyroid lesions than neck ultrasound in approximately 50% patients. To the best of our knowledge, this is the first study investigating the diagnostic performance and clinical utility of F-18 fluorocholine PET/CT in a uniform cohort with secondary or tertiary hyperparathyroidism.

Compared with primary hyperparathyroidism, secondary and tertiary hyperparathyroidism exhibit different disease features, including a higher prevalence of multiglandular

disease, higher frequency of glandular hyperplasia rather than adenoma, and smaller diseased parathyroid glands [19, 25, 27, 34, 35]. Primary hyperparathyroidism presents with a single, enlarged parathyroid adenoma in approximately 85% of cases [16, 17, 25, 27]. Owing to these differences, the diagnostic performance of Tc-99m sestamibi scan varies between cases of primary and secondary/tertiary hyperparathyroidism in the literature. The sensitivity of Tc-99m sestamibi scan for primary hyperparathyroidism can reach 70–80%, while its sensitivity in patients with secondary or tertiary hyperparathyroidism is lower and is reported around 40–60% [15–17, 26]. Studies have shown that the detection rate of F-18 fluorocholine PET/CT for primary hyperparathyroidism is between 94 and 100%, which is significantly superior to that of the traditional imaging modalities (Table 3) [19–24, 30, 31, 34, 36–38]. However, whether F-18 fluorocholine PET/CT maintains a high sensitivity for the detection of small and multiglandular hyperparathyroid lesions in secondary or tertiary hyperparathyroidism is unknown. In our study, the majority of our patients had multiglandular disease, and the median weight of the lesions (557 mg) was smaller than that in primary hyperparathyroidism (1000 mg, Table 3). Although Tc-99m sestamibi scan has a low sensitivity of 55%, F-18 fluorocholine PET/CT still demonstrated a high sensitivity of 86%, which is comparable with the results in primary hyperparathyroidism [19, 25, 27, 35]. Based on the findings from our study and present literature, we suggest that the diagnostic performance of F-18 fluorocholine PET/CT is not influenced by different disease features between primary and secondary/tertiary hyperparathyroidism. F-18 fluorocholine PET/CT shows a consistently higher sensitivity than Tc-99m sestamibi scan in the detection of hyperfunctioning parathyroid glands.

In secondary or tertiary hyperparathyroidism, early surgical failure with persistent disease may occur in 5–10% of patients, and the recurrence rate reaches 20–30% at 5 years [39, 40]. The surgical procedure for secondary/tertiary hyperparathyroidism is more extensive and more likely to dissect near-critical neurovascular structures than the focused parathyroidectomy of primary hyperparathyroidism [2, 5, 41]. Therefore, a preoperative image accurately illustrating the location and number of abnormal glands is helpful. Tc-99m sestamibi scans show low sensitivity for secondary/tertiary hyperparathyroidism lesions and usually fail to provide additional information if neck ultrasound has been done [14, 16–18, 26, 42–44]. Instead, our data suggest that F-18 fluorocholine PET/CT identifies more hyperplastic parathyroid lesions than neck ultrasound and that approximately 50% of the patients who have undergone neck ultrasounds would benefit from additional F-18 fluorocholine PET/CT, for a more accurate and sophisticated surgical planning. In secondary or tertiary hyperparathyroidism, a missed parathyroid gland may be the cause of a difficult and extensive reoperation. Extensive surgical dissection would increase operative time and also increase the risk of morbidity (recurrent laryngeal nerve injury, hematoma, or hypoparathyroidism). In our study, the surgeon did report a

Table 3 Studies using radioactive choline PET for patients with hyperparathyroidism

Source	Design	Diagnosis	Radiotracer	Case, no	Lesion, no	Glandular weight (mg), median	Sensitivity (%)		
							Choline PET	Tc-99m sestamibi	Ultrasound
Araz et al. (2018) [32]	Pro	Primary	F-18 choline	35	NA	NA	96 (p)	78 (p)	NA
Becheshti et al. (2018)[a] [19]	Pro	Primary	F-18 choline	100	277	1000	94 (l)	61 (l)	NA
Rep et al. (2018) [36]	Pro	Primary	F-18 choline	36	41	NA	97 (l)	64 (l)	NA
Hocevar et al. (2017) [35]	Retro	Primary	F-18 choline	151	NA	NA	99 (p)	NA	NA
Thanseer et al. (2017) [30]	Pro	Primary	F-18 choline	54	56	1000	100 (l)/100 (p)	76 (l)/81 (p)	69 (l)/69 (p)
Rep et al. (2015) [34]	Pro	Primary	F-18 choline	43	NA	NA	95[b]	NA	NA
Our study	Pro	Secondary/tertiary	F-18 choline	30	116	577	86 (l)[c]	55 (l)[c]	62 (l)[c]

PET positron emission tomography, *Pro* prospective, *Retro* retrospective, *(p)* patient-based analysis, *(l)* lesion-based analysis, *NA* not available

[a]Thirty-three patients received Tc-99m tetrofosmin scintigraphy instead of Tc-99m sestamibi scans

[b]No report of patient-based or lesion-based sensitivities

[c]Diagnostic performance based on 27 patients

reduced surgical time or an increased confidence for lesion localization with the aid of F-18 fluorocholine PET/CT. Figure 2 shows a case that benefited from the F-18 fluorocholine PET/CT because of the identification of a right upper hyperplastic parathyroid gland. The upper or superior glands are usually localized at the level of the thyrolaryngeal groove, a site explorable by ultrasonography with some difficulty. In addition, upper glands are just behind the thyroid lobes and closed to the thick thyroid tissue, which makes identification by the traditional scintigraphy difficult.

The improved sensitivity of F-18 fluorocholine PET/CT when compared with that of Tc-99m sestamibi scans in secondary/tertiary hyperparathyroidism is partially attributed to a better image contrast and spatial resolution of the PET machine [45]. The spatial resolution of the PET machine is approximately 5 mm [46]; in contrast, that of SPECT is considerably larger, reported to be approximately 15 mm [47]. Another reason is that F-18 fluorocholine and Tc-99m sestamibi exhibit different radiotracer uptake mechanisms [17, 48]. Tc-99m sestamibi mainly concentrates on the mitochondria-rich oxyphil cells, which are abundant in the adenoma of primary hyperparathyroidism. The Tc-99m sestamibi scan has a lower detection rate in secondary or tertiary hyperparathyroidism, because the diseased parathyroid gland is characterized by chief cell hyperplasia instead of oxyphil proliferation [16, 17, 25]. The increased uptake of F-18 fluorocholine in the lesion of hyperparathyroidism is due to the upregulation of the phospholipid-dependent choline kinase pathway [23].

In our study, the NPVs of Tc-99m sestamibi scan and PET/CT were suboptimal. The NPV of Tc-99m sestamibi scan was 23%, which is similar to the previous reports (0–35%) [15]. F-18 fluorocholine PET/CT had a higher NPV of 52%. Nevertheless, the low NPV may not affect the extent of bilateral neck dissection of parathyroidectomy. Further study is required to confirm this finding.

Traditionally, Tc-99m sestamibi scintigraphy has a sensitivity approximating 90% when the parathyroid lesion is ≥ 300 mg [27]. The sensitivity of F-18 fluorocholine PET/CT in our study exceeded 90% for parathyroid lesions ≥ 175 mg, and reached 95% for those ≥ 200 mg.

We further analyzed the semiquantitative parameters of F-18 fluorocholine PET. The SUVmax of the lesion in the early and delayed images showed no significant difference. Nevertheless, the *P/T* values were significantly higher in the delayed images than in the early images. Our findings are in line with the data reported by Broos et al. [29], suggesting that the delayed image allows better thyroid background washout and may achieve a better lesion contrast. However, our data only showed a slightly increased sensitivity for the delayed image without statistical significance.

We are aware of the limitations of our study. First, our study population was relatively small, and may have caused biases to the statistical analysis. Second, this was a single-center study. A multicenter study may improve the generalizability. Finally, the analysis of the correlation between semiquantitative F-18 fluorocholine PET parameters and lesion weight in our study is preliminary. Further research is required to examine the clinical benefit of semiquantitative F-18 fluorocholine PET parameters.

Conclusion

Currently, neck ultrasound is the preferred preoperative imaging in patients with secondary/tertiary hyperparathyroidism, and the use of Tc-99m sestamibi scan is limited in these patients. Our data indicate that F-18 fluorocholine PET/CT shows a high diagnostic power and can supersede Tc-99m sestamibi scan for preoperative evaluation. F-18 fluorocholine PET/CT identified more hyperplastic parathyroid lesions in approximately 50% patients who had received neck ultrasounds. Therefore, it may complement neck ultrasound in preoperative assessment and enable a better surgical planning in secondary or tertiary hyperparathyroidism.

Compliance with ethical standards

References

1. Al Zahrani A, Levine MA. Primary hyperparathyroidism. Lancet. 1997;349:1233–8.
2. van der Plas WY, Noltes ME, van Ginhoven TM, Kruijff S. Secondary and tertiary hyperparathyroidism: a narrative review. Scand J Surg. 2019. https://doi.org/10.1177/1457496919866015.
3. Liyanage T, Ninomiya T, Jha V, Neal B, Patrice HM, Okpechi I, et al. Worldwide access to treatment for end-stage kidney disease: a systematic review. Lancet. 2015;385:1975–82.
4. Tang SCW, Yu X, Chen HC, Kashihara N, Park HC, Liew A, et al. Dialysis care and dialysis funding in asia. Am J Kidney Dis. 2019. https://doi.org/10.1053/j.ajkd.2019.08.005.
5. Hindie E, Zanotti-Fregonara P, Tabarin A, Rubello D, Morelec I, Wagner T, et al. The role of radionuclide imaging in the

surgical management of primary hyperparathyroidism. J Nucl Med. 2015;56:737–44.

6. Trombetti A, Christ ER, Henzen C, Gold G, Brandle M, Herrmann FR, et al. Clinical presentation and management of patients with primary hyperparathyroidism of the Swiss Primary Hyperparathyroidism Cohort: a focus on neuro-behavioral and cognitive symptoms. J Endocrinol Invest. 2016;39:567–76.

7. Fraser WD. Hyperparathyroidism. Lancet. 2009;374:145–58.

8. Moorthi RN, Moe SM. CKD-mineral and bone disorder: core curriculum 2011. Am J Kidney Dis. 2011;58:1022–36.

9. Tang JA, Friedman J, Hwang MS, Salapatas AM, Bonzelaar LB, Friedman M. Parathyroidectomy for tertiary hyperparathyroidism: a systematic review. Am J Otolaryngol. 2017;38:630–5.

10. Yang J, Hao R, Yuan L, Li C, Yan J, Zhen L. Value of dual-phase (99m)Tc-sestamibi scintigraphy with neck and thoracic SPECT/CT in secondary hyperparathyroidism. AJR Am J Roentgenol. 2014;202:180–4.

11. Taieb D, Urena-Torres P, Zanotti-Fregonara P, Rubello D, Ferretti A, Henter I, et al. Parathyroid scintigraphy in renal hyperparathyroidism: the added diagnostic value of SPECT and SPECT/CT. Clin Nucl Med. 2013;38:630–5.

12. Jones BA, Lindeman B, Chen H. Are Tc-99m-sestamibi scans in patients with secondary hyperparathyroidism and renal failure needed? J Surg Res. 2019;243:380–3.

13. Alkhalili E, Tasci Y, Aksoy E, Aliyev S, Soundararajan S, Taskin E, et al. The utility of neck ultrasound and sestamibi scans in patients with secondary and tertiary hyperparathyroidism. World J Surg. 2015;39:701–5.

14. Zhen L, Li H, Liu X, Ge BH, Yan J, Yang J. The application of SPECT/CT for preoperative planning in patients with secondary hyperparathyroidism. Nucl Med Commun. 2013;34:439–44.

15. Caldarella C, Treglia G, Pontecorvi A, Giordano A. Diagnostic performance of planar scintigraphy using (9)(9)mTc-MIBI in patients with secondary hyperparathyroidism: a meta-analysis. Ann Nucl Med. 2012;26:794–803.

16. Kettle AG, O'Doherty MJ. Parathyroid imaging: how good is it and how should it be done? Semin Nucl Med. 2006;36:206–11.

17. Palestro CJ, Tomas MB, Tronco GG. Radionuclide imaging of the parathyroid glands. Semin Nucl Med. 2005;35:266–76.

18. Fuster D, Ybarra J, Ortin J, Torregrosa JV, Gilabert R, Setoain X, et al. Role of pre-operative imaging using 99mTc-MIBI and neck ultrasound in patients with secondary hyperparathyroidism who are candidates for subtotal parathyroidectomy. Eur J Nucl Med Mol Imaging. 2006;33:467–73.

19. Beheshti M, Hehenwarter L, Paymani Z, Rendl G, Imamovic L, Rettenbacher R, et al. (18)F-Fluorocholine PET/CT in the assessment of primary hyperparathyroidism compared with (99m)Tc-MIBI or (99m)Tc-tetrofosmin SPECT/CT: a prospective dual-centre study in 100 patients. Eur J Nucl Med Mol Imaging. 2018;45:1762–71.

20. Quak E, Blanchard D, Houdu B, Le Roux Y, Ciappuccini R, Lireux B, et al. F18-choline PET/CT guided surgery in primary hyperparathyroidism when ultrasound and MIBI SPECT/CT are negative or inconclusive: the APACH1 study. Eur J Nucl Med Mol Imaging. 2018;45:658–66.

21. Treglia G, Piccardo A, Imperiale A, Strobel K, Kaufmann PA, Prior JO, et al. Diagnostic performance of choline PET for detection of hyperfunctioning parathyroid glands in hyperparathyroidism: a systematic review and meta-analysis. Eur J Nucl Med Mol Imaging. 2019;46:751–65.

22. Broos WAM, van der Zant FM, Knol RJJ, Wondergem M. Choline PET/CT in parathyroid imaging: a systematic review. Nucl Med Commun. 2019;40:96–105.

23. Boccalatte LA, Higuera F, Gomez NL, de la Torre AY, Mazzaro EL, Galich AM, et al. Usefulness of 18F-fluorocholine positron emission tomography-computed tomography in locating lesions in hyperparathyroidism: a systematic review. JAMA Otolaryngol Head Neck Surg. 2019. https://doi.org/10.1001/jamaoto.2019.0574.

24. Michaud L, Balogova S, Burgess A, Ohnona J, Huchet V, Kerrou K, et al. A pilot comparison of 18F-fluorocholine PET/CT, ultrasonography and 123I/99mTc-sestaMIBI dual-phase dual-isotope scintigraphy in the preoperative localization of hyperfunctioning parathyroid glands in primary or secondary hyperparathyroidism: influence of thyroid anomalies. Medicine (Baltimore). 2015;94:e1701.

25. Duan K, Gomez Hernandez K, Mete O. Clinicopathological correlates of hyperparathyroidism. J Clin Pathol. 2015;68:771–87.

26. Pham TH, Sterioff S, Mullan BP, Wiseman GA, Sebo TJ, Grant CS. Sensitivity and utility of parathyroid scintigraphy in patients with primary versus secondary and tertiary hyperparathyroidism. World J Surg. 2006;30:327–32.

27. Ziessman HA, O'Malley JP, Thrall JH, Fahey FH. Nuclear medicine: the requisites. Philadelphia: Elsevier Saunders; 2014. p. 97.

28. DeGrado TR, Reiman RE, Price DT, Wang S, Coleman RE. Pharmacokinetics and radiation dosimetry of 18F-fluorocholine. J Nucl Med. 2002;43:92–6.

29. Broos WAM, Wondergem M, van der Zant FM, Knol RJJ. Dual-time-point (18)F-fluorocholine PET/CT in parathyroid imaging. J Nucl Med. 2019;60:1605–10.

30. Rep S, Hocevar M, Vaupotic J, Zdesar U, Zaletel K, Lezaic L. (18)F-choline PET/CT for parathyroid scintigraphy: significantly lower radiation exposure of patients in comparison to conventional nuclear medicine imaging approaches. J Radiol Prot. 2018;38:343–56.

31. Hocevar M, Lezaic L, Rep S, Zaletel K, Kocjan T, Sever MJ, et al. Focused parathyroidectomy without intraoperative parathormone testing is safe after pre-operative localization with (18)F-Fluorocholine PET/CT. Eur J Surg Oncol. 2017;43:133–7.

32. Chou FF, Lee CH, Chen JB, Hsu KT, Sheen-Chen SM. Intraoperative parathyroid hormone measurement in patients with secondary hyperparathyroidism. Arch Surg. 2002;137:341–4.

33. Kim WY, Lee JB, Kim HY. Efficacy of intraoperative parathyroid hormone monitoring to predict success of parathyroidectomy for secondary hyperparathyroidism. J Korean Surg Soc. 2012;83:1–6.

34. Thanseer N, Bhadada SK, Sood A, Mittal BR, Behera A, Gorla AKR, et al. Comparative effectiveness of ultrasonography, 99mTc-sestamibi, and 18F-fluorocholine PET/CT in detecting parathyroid adenomas in patients with primary hyperparathyroidism. Clin Nucl Med. 2017;42:e491–e497497.

35. Fang L, Tang B, Hou D, Meng M, Xiong M, Yang J. Relationship between parathyroid mass and parathyroid hormone level in hemodialysis patients with secondary hyperparathyroidism. BMC Nephrol. 2015;16:82.

36. Araz M, Soydal C, Ozkan E, Kir MK, Ibis E, Gullu S, et al. The efficacy of fluorine-18-choline PET/CT in comparison with 99mTc-MIBI SPECT/CT in the localization of a hyperfunctioning parathyroid gland in primary hyperparathyroidism. Nucl Med Commun. 2018;39:989–94.

37. Lezaic L, Rep S, Sever MJ, Kocjan T, Hocevar M, Fettich J. (1)(8)F-Fluorocholine PET/CT for localization of hyperfunctioning parathyroid tissue in primary hyperparathyroidism: a pilot study. Eur J Nucl Med Mol Imaging. 2014;41:2083–9.

38. Rep S, Lezaic L, Kocjan T, Pfeifer M, Sever MJ, Simoncic U, et al. Optimal scan time for evaluation of parathyroid adenoma with [(18)F]-fluorocholine PET/CT. Radiol Oncol. 2015;49:327–33.

39. Mazzaferro S, Pasquali M, Farcomeni A, Vestri AR, Filippini A, Romani AM, et al. Parathyroidectomy as a therapeutic tool for targeting the recommended NKF-K/DOQI ranges for serum calcium, phosphate and parathyroid hormone in dialysis patients. Nephrol Dial Transplant. 2008;23:2319–23.

40. Kovacevic B, Ignjatovic M, Zivaljevic V, Cuk V, Scepanovic M, Petrovic Z, et al. Parathyroidectomy for the attainment of NKF-K/DOQI and KDIGO recommended values for bone and mineral metabolism in dialysis patients with uncontrollable secondary hyperparathyroidism. Langenbecks Arch Surg. 2012;397:413–20.

41. Judson BL, Shaha AR. Nuclear imaging and minimally invasive surgery in the management of hyperparathyroidism. J Nucl Med. 2008;49:1813–8.

42. de la Rosa A, Jimeno J, Membrilla E, Sancho JJ, Pereira JA, Sitges-Serra A. Usefulness of preoperative Tc-mibi parathyroid scintigraphy in secondary hyperparathyroidism. Langenbecks Arch Surg. 2008;393:21–4.

43. Gasparri G, Camandona M, Bertoldo U, Sargiotto A, Papotti M, Raggio E, et al. The usefulness of preoperative dual-phase 99mTc MIBI-scintigraphy and IO-PTH assay in the treatment of secondary and tertiary hyperparathyroidism. Ann Surg. 2009;250:868–71.

44. Udelsman R, Akerstrom G, Biagini C, Duh QY, Miccoli P, Niederle B, et al. The surgical management of asymptomatic primary hyperparathyroidism: proceedings of the Fourth International Workshop. J Clin Endocrinol Metab. 2014;99:3595–606.

45. Slomka PJ, Miller RJH, Hu LH, Germano G, Berman DS. Solid-state detector SPECT myocardial perfusion imaging. J Nucl Med. 2019;60:1194–204.

46. van der Vos CS, Koopman D, Rijnsdorp S, Arends AJ, Boellaard R, van Dalen JA, et al. Quantification, improvement, and harmonization of small lesion detection with state-of-the-art PET. Eur J Nucl Med Mol Imaging. 2017;44:4–16.

47. Imbert L, Poussier S, Franken PR, Songy B, Verger A, Morel O, et al. Compared performance of high-sensitivity cameras dedicated to myocardial perfusion SPECT: a comprehensive analysis of phantom and human images. J Nucl Med. 2012;53:1897–903.

48. Kirienko M, Sollini M, Lopci E, Versari A, Chiti A. Applications of PET imaging with radiolabelled choline (11C/18F-choline). Q J Nucl Med Mol Imaging. 2015;59:83–94.

Affiliations

Yu-Hung Chen[1] · Hwa-Tsung Chen[2] · Ming-Che Lee[2] · Shu-Hsin Liu[1,3] · Ling-Yi Wang[4,5] · Kun-Han Lue[3] · Sheng-Chieh Chan[1]

1   Department of Nuclear Medicine, Hualien Tzu Chi Hospital, Buddhist Tzu Chi Medical Foundation, Hualien, Taiwan

2   Department of Surgery, Hualien Tzu Chi Hospital, Buddhist Tzu Chi Medical Foundation, Hualien, Taiwan

3   Department of Medical Imaging and Radiological Sciences, Tzu Chi University of Science and Technology, Hualien, Taiwan

4   Epidemiology and Biostatistics Consulting Center, Department of Medical Research, Hualien Tzu Chi Hospital, Buddhist Tzu Chi Medical Foundation, Hualien, Taiwan

5   Department of Pharmacy, Hualien Tzu Chi Hospital, Buddhist Tzu Chi Medical Foundation, Hualien, Taiwan